J. Indian Inst. Sci., Nov.–Dec. 2006, **86**, 797–803

Short Communication

Charge-ordering in quarter-filled low-dimensional conductors: Implications of long-range Coulomb interactions

SWAPAN K. PATI
Theoretical Sciences Unit, Jawharlal Nehru Center for Advanced Scientific Research, Jakkur Campus, Bangalore 560 064, India. email: pati@jncasr.ac.in

Received on November 18, 2004; Revised on October 5, 2005.

Abstract

We investigate the charge-ordering (CO) in quasi one-dimensional Pariser–Parr–Pople model at quarter filling where the longer-range Coulomb interactions and dimerization in the hopping integrals are included. The inter-site electron repulsion integrals have been incorporated using the interpolation formulae given by Ohno. We find that while the longer-range interactions stabilize the CO phase, dimerization suppresses its stability. Using an exact diagonalization scheme for small cluster sizes, we determine the zero-temperature charge-ordering phase boundary in the model parameter space. The realistic parameter values for the low-dimensional Bechgaard salts are found to exist within the CO phase boundary. We conjecture that the true longer-range electron–electron interactions are necessary to account for the CO phase in these organic systems.

Keywords: Charge-ordering, Coulomb interactions, electron repulsion integrals, Bechgaard salts.

1. Introduction

In last decade, there has been a renewed interest on charge-ordering of organic charge-transfer complexes [1–4]. It has been the subject of many interesting theoretical and experimental papers. Charge-ordering (CO) is a phenomenon in which the systems undergo a quantum phase transition where the electrons are localized at atomic or lattice sites. The role of electron–electron and electron–phonon interactions on this charge-ordering phase transition has been studied quite extensively [5–10]. While the electron–phonon coupling gives rise to the usual $2k_F$ (k_F is the Fermi wave vector) Peierls instability, the electron–electron interaction is believed to be most responsible for localization of electrons. Additionally in the CO phase, the electronic spin degrees of freedom can undergo yet another phase transition as the temperature is lowered. This magnetic transition gives rise to a large number of magnetic phases, including ordered antiferromagnetic (AF), spin–density wave (SDW) and spin–Peierls (SP) phases [11].

There exist a large number of quasi-one-dimensional systems, where the details of structures can fundamentally influence the low-temperature physics. Among those, the isostructural M_2X complexes, often referred to as Bechgaard salts, where M is tetramethyltetrathiofulvalene (TMTTF), or tetramethyltetraseleenafulvalene (TMTSF), offer the richest opportunities to study various phase transitions. The counter ions X can be PF_6, AsF_6, ClO_4 and SbF_6. TMTTF has been shown to exist in one dimension with extremely small interchain

coupling [12], while for TMTSF the interchain coupling is moderately strong. It is found that the lattice dimerization in the system causes an alternation of transfer integrals, which in turn opens up a gap in the excitation spectrum. This is the Peierls mechanism of metal insulator transition. This transition in these Bechgaard salts is then controlled by the small interchain hopping to emphasize a possible mechanism for dimensional crossover (from 1- to 2-dimension) [13, 14].

As has been mentioned before, these are truly one-dimensional systems with negligible inter-chain interactions. NMR [15] and dielectric response [16] measurements have suggested possible charge-ordering phase transitions in these materials. Charge-ordering in this case divides the system into nonequivalent charged species at a temperature corresponding to T_{co}. This transition temperature is different for different systems, $T_{co} = 70$ K for X = PF_6, $T_{co} = 100$ K for X = AsF_6 and $T_{co} = 154$ K for X = SbF_6 [17]. What is interesting is that in all the cases, the transition temperature is much higher than that corresponding to the electronic transition associated with the organic systems ($T \sim 1 - 30$ K). Most importantly, experiments on these systems suggest that the CO transition is the consequence of Coulomb interactions, as no evidence of structural anomaly or molecular reorientation in the transition region has been observed [15].

These materials thus provide a very suitable ground for studying one-dimensional correlated electronic system at quarter-filling. There exist a large number of theoretical studies on the 1D quarter-filled Hubbard and extended Hubbard models, which provide useful insight to consider the physics of CO transition. In general, Coulomb interactions are believed to give rise to $4k_F$ charge density wave (CDW) instabilities, while the lattice dimerization leads to $2k_F$ charge disproportionations [6, 18, 19]. Recent calculations on models including lattice dimerizations have shown that both the $2k_F$ and $4k_F$ CDW instabilities can coexist with $2k_F$ SDW instabilities in the ground state of the system [18, 20]. We note however that most of these studies do not consider models where interactions are truly long-ranged. Furthermore, these models have been solved mostly by mean-field or its modified versions [21].

It is quite well known that the mean-field solutions of strongly interacting systems can lead to overestimation of the stability of the ordered phases. Organic charge-transfer salts or transition metal oxides are known to be highly interacting systems, where long-ranged electron–electron interactions are essential to account for any phase transitions, while the mean-field solution cannot be used for longer-ranged electron–electron interactions. In this context, exact diagonalization of small system sizes and density–matrix–renormalization method have been rigorously used to invalidate such mean-field solutions [20, 21].

In this paper, we study the charge-ordering within a one-dimensional long-ranged Pariser–Parr–Pople (PPP) model Hamiltonian at quarter-filling with dimerization in hopping integrals. The PPP model has been the standard model for a serious study of the electronic states of organic systems. An exact diagonalization scheme is implemented for solving the systems with 16 lattice sites. We contrast and compare our results with the results obtained using the Hubbard model and also mean-field solutions by others. Finally, we implicate some of our results to the charge-order phase observed in organic conductors.

2. Model Hamiltonian

The PPP Hamiltonian is defined by the Hamiltonian

$$H = t\sum_{i\sigma}[(1+(-\delta)^i)c^{\dagger}_{i\sigma}c_{i+1\sigma} + HC] + U\sum_{i\sigma} n_{i\sigma}n_{i-\sigma} + \sum_{i>j} V_{ij}n_i n_j \tag{1}$$

where dimerization δ is included in transfer (t) parameters. U is the Hubbard onsite repulsion energy and V_{ij} are the offsite PPP repulsion integrals. Number operators, $n_i = c_i^{\dagger}c_i$ counts the number of electrons at site i. Note that we recover the Hubbard model when all the V_{ij} with $i \neq j$ are set to zero.

In keeping with the spirit of phenomenology associated with the PPP Hamiltonian, the integrals, V_{ij}, are interpolated smoothly between U for zero inter-site separation and e^2/r_{12} for the inter-site separation tending to infinity and explicit evaluation of the repulsion integrals is thus bypassed. The most widely used interpolation formulae given by Ohno has been incorporated in our study [22]. In this interpolation scheme, the inter-site electron repulsion integrals, V_{ij}, are given by:

$$V_{ij} = 14.397\left[\frac{28.794}{(U_i+U_j)^2} + r_{ij}^2\right]^{-1/2} \tag{2}$$

where r_{ij} is the distance between sites i and j. Note that in all the cases, it is assumed that r_{ij} is in Å, and U and V_{ij} are in eV. Bond alternation parameter δ, introduced in the Hamiltonian above has an alternate effect on the bond distances. In all our calculations, we have considered the nearest neighbor bond distance r_{12} to be 1 Å and the transfer term $t = 1$, for $\delta = 0$, and the proportional change from the uniform values when δ is nonzero. Therefore, we have two parameters to vary, U and δ.

We have calculated charge density ($\langle n_i \rangle$) and bond-order, ($\langle p_k \rangle$), at every site, i and at every bond, k, respectively. They are defined as

$$\begin{aligned} \langle n_i \rangle &= \left\langle \sum_{\sigma} c^{\dagger}_{i\sigma}c_{i\sigma} \right\rangle \\ \langle p_i \rangle &= \left\langle \sum_{\sigma} c^{\dagger}_{i\sigma}c_{i+1\sigma} \right\rangle \end{aligned} \tag{3}$$

For very small U and δ values, the ground state of 16 sites ring remains degenerate. In such a situation, we have obtained 2×2 matrices both for charge-density and bond-order, corresponding to two degenerate states. After diagonalizing these matrices, we compare the eigenvectors corresponding to two sets of eigenvalues associated with each site/bond. We then choose one set of eigenvalues which can be simultaneously observed. As the system is quarter-filled, $4k_F$ instabilities correspond to two-fold periodicity, while the $2k_F$ instabilities correspond to systems with four-fold disproportions. We shall show below that the long-range correlations can lead to $2k_F$ CDW in the realistic electronic parameters regime for quasi-1D quarter-filled Bechgaard salts. Thus our results suggest that the true longer-range electron–electron interactions are essential to account for the CO phase observed in these materials.

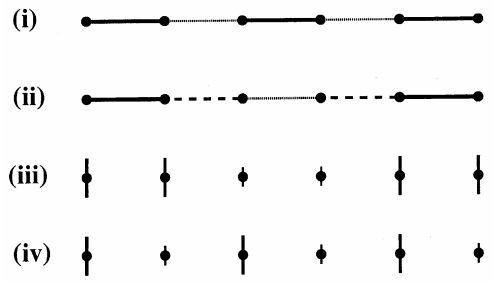

FIG. 1. Schematic configurations of the quarter-filled one-dimensional (i) $4k_F$ BOW, (ii) $2k_F$ BOW, (iii) $2k_F$ CDW, and (iv) $4k_F$ CDW phases. The thick bonds are strong, while dotted and broken bonds are weak and of intermediate strengths, respectively. The sizes of the vertical lines on sites give their relative charge densities.

3. Results and discussion

We shall analyze two typical cases. First is the case for the paramagnetic state where the charge density distribution is uniform. In the second case, the charge density oscillates with a particular periodicity. In case of bond-order oscillations, these two phases have different ordering. Some possible broken symmetry phases are drawn in Fig. 1. In the following, we identify these phases and derive a phase boundary in the δ–U plane.

Let us first analyze our results for charge density and bond-order distribution in PPP and Hubbard rings of 16 sites. For small bond alternation, δ, and small Hubbard repulsion, U, $\langle n_i \rangle$ and $\langle p_i \rangle$ are shown in Fig. 2. The contrasting behaviors between Hubbard and long-ranged correlated models can be clearly seen in the figure. The charge densities for the Hubbard model show no oscillations, while for the PPP model, they develop an oscillatory pattern with four-fold periodicity, which corresponds to $2k_F$ instabilities as it is for 1/4 filled system. The bond-orders also show similar behaviors. In case of PPP model, the bond-orders alternate with $2k_F$ periodicity, while the bond strengths have alternate strong and weak characters for the Hubbard model. It has been established that the bond-order oscillations have the form $\Delta r_i \propto [K_2 \cos(2k_F - \phi_2) + K_4 \cos(4k_F - \phi_4)]$, where K_2 and K_4 are the relative weights of the $2k_F$ and $4k_F$ components, respectively, and ϕs are the phase factors [5]. However, the CDW oscillation can either have the $2k_F$ or $4k_F$ modulations. But our calculations with long-range Coulomb interactions establish that the bond-order oscillations have either $2k_F$ or $4k_F$ instabilities but not both. However, the CDW oscillations either have $2k_F$ oscillations or no oscillations.

In Fig. 3, we plot the $\langle n_i \rangle$ and $\langle p_i \rangle$ for two different U values but with the same δ for the PPP model. With small U values, as discussed earlier, both CDW and BOW have $2k_F$ oscillations. However, for large U parameters, the BOW acquires $4k_F$ oscillations while the charge density remains uniform. This is similar to the results obtained for the Hubbard model, although the BOW oscillations in the PPP model have stronger oscillations compared to the same for the Hubbard model. This is quite easy to understand, as the large U PPP model essentially localizes the electrons as the case with large U Hubbard. Moreover, Hubbard U has long been recognized to give rise to bond-strength alternations and in the case of the PPP model as the correlation is large and long-ranged, the bond-strength alternations are large and dominant.

It is quite clear that there are two types of phases that can exist in a long-ranged correlated Hamiltonian as functions of correlation strengths and dimerizations. Next we derive

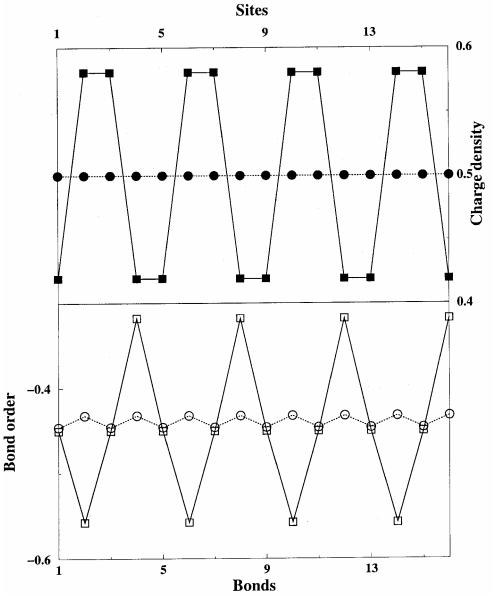

FIG. 2. Charge-density distribution and bond-order profiles are shown as a function of sites and bonds, respectively. Squares represent results for PPP model and the circles for the Hubbard model. For both the cases, $U = 1$ and $\delta = 0.05$.

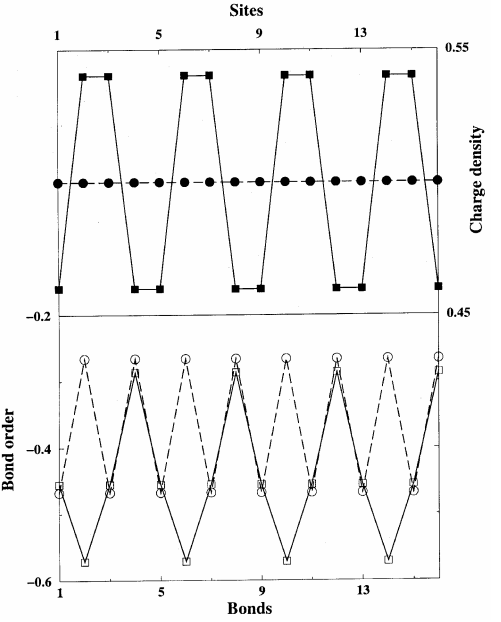

FIG. 3. Charge-density and bond-order data for the PPP model as a function of sites and bonds, respectively. Results are shown for $U = 2$ (squares) and $U = 10$ (circles). For charge density, $\delta = 0.25$ and for bond-order, $\delta = 0.1$.

the phase boundaries between these two phases. We have carried out calculations for a large number of points in the two-dimensional phase space, with varying U and δ. The phase boundary is shown in Fig. 4. Note that, with increase in δ, the long-range correlations do not play almost any role. This is because, the large δ introduces strong alternations in transfer integrals as well as in the distances, r_{ij}. As the long-ranged interactions depend strongly on the distance, in the limit of large δ, the long-ranged interactions reduce to only a few neighbors. Considering just the nearest-neighbor short-ranged interactions, in the limit

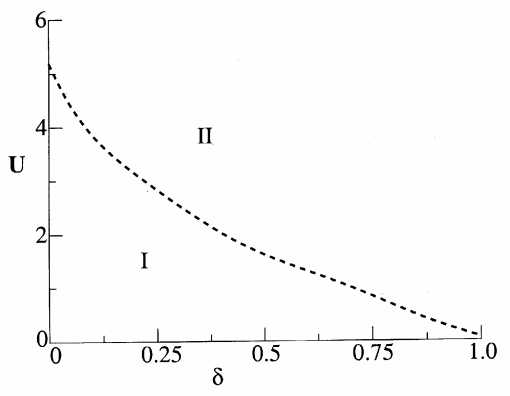

Fig. 4. Phase diagram in the Hubbard U and dimerization parameter (δ) space. The CO phase boundary is shown by the dashed line. The lower-left side of the boundary (I) is the CO phase, and the upper-right side (II) is the paramagnetic phase.

$U \to \infty$, the system becomes equivalent to a spin chain, where a dimer can be expressed as a pseudo-spin. In this model, the CO can be visualized as the phase where quantum fluctuation of the dimer electron is less compared to the inter-dimer interactions. For large δ, the transfer integral in the dimer becomes large compared to inter-dimer interactions. This suggests that the strong dimerizations should suppress the stability of the CO phase, which is the case as shown in our phase diagram. Essentially, at $\delta = 1$, the chain is completely decoupled and transfer term reduces only to nearest-neighbors.

We shall now compare our results with some of the previous calculations in this field. Earlier calculations on correlated Hamiltonians were based on either Hubbard or extended Hubbard Hamiltonians. Hubbard Hamiltonian, as we have discussed does not give rise to CO phase at all. However, the extended Hubbard Hamiltonians with a nearest-neighbor electron–electron interaction strength (V) stabilizes the CO phase. The CDW oscillation corresponds to $4k_F$ instability and the CO phase appears at around $U > 2V$ even for large alternation in hopping integrals [21]. Our results on the other hand suggest a $2k_F$ CDW instability and the CO phase exists for the whole range of bond alternation parameters ($0 \le \delta < 1$) and for a U value of little above 5 eV when there is no bond alternation, to a U value close to zero for very large bond alternations.

Let us now briefly consider the experimental implications of our results. Estimation of parameter values for real materials has given U values ranging from 5 to 10 eV. For example, U in units of hopping integral is 5.0 eV for $(TMTSF)_2ClO_4$ and 7.0 eV for $(TMTTF)_2PF_6$. The dimerization strengths also vary from one system to the other. A careful estimation suggests that the dimerization is $\delta \sim 0.18$ for $(TMTTF)_2PF_6$ and is as low as 0.05 for $(TMTSF)_2ClO_4$ [21, 23]. Dimerizations for the other systems are within this range. These values of the parameters in our phase diagram are thus located within the CO phase, far apart from the uniform phase boundary. Note that, this CO phase exists at temperature, $T = 0$ K, suggesting the existence of CO phase at $T > 0$ K when the presence of higher dimensional couplings are considered. It is beyond doubt that the large T_{co} observed in these materials is suggestive of rather strong interchain coupling via longer-range electron–electron interactions.

4. Conclusions

To conclude, we have considered charge ordering in a quasi one-dimensional chain with longer-ranged Coulomb interactions and dimerization in the hopping parameters, at quarter-filling. Ohno's interpolation scheme for the electron repulsion integrals has been incorporated. At zero-temperature, we have obtained the phase boundary for the stabilization of the charge-ordered phase, using an exact diagonalization method. Our results suggest that the CO phase is stabilized due to longer-ranged Coulomb interactions, and the parameters for the quasi one-dimensional organic Bechgaard salts are well inside the CO phase boundary. We have argued that the true longer-ranged Coulomb interactions are essential to account for CO phases in these quasi-one-dimensional organic salts.

Acknowledgements

I thank Dr Y. Anusooya and Prof. S. Ramasesha for fruitful discussions and DST, Govt. of India for funding.

References

1. T. Sasaki, and N. Toyota, *Phys. Rev. B,* **49**, 10120–10126 (1994).
2. J. Caulfield *et al*., *Phys. Condens. Matter*, **6**, L155–158 (1994).
3. J. P. Pouget, and S. Ravy, *J. Phys. 1*, **6**, 1501 (1996); *Synth. Met.*, **85**, 1523–1529 (1997).
4. K. Miyagawa, A. Kawamoto, and K. Kanoda, *Phys. Rev. B*, **56**, R8487–8490 (1997).
5. K. C. Ung, S. Mazumdar, and D. Toussaint, *Phys. Rev. Lett.*, **73**, 2603–2606 (1994).
6. H. Seo, and H. Fukuyama, *J. Phys. Soc. Jap*., **66**, 1249–1254 (1997).
7. N. Kobayashi, and M. Ogata, *J. Phys. Soc. Jap*., **66**, 3356–3360 (1997).
8. R. T. Clay, A. W. Sandvik, and D. K. Campbell, *Phys. Rev. B*, **59**, 4665–1669 (1999).
9. H. Yostioka, M. Tsuchiizu and Y. Suzumura, *J. Phys. Soc. Jap*., **69**, 651–655 (2000).
10. M. Nakamura, *Phys. Rev. B*, **61**, 16377–16381 (2000).
11. D. Jerome, in *Organic conductors* (J. P. Farges, ed.), p. 405, Marcel Dekker (1994); D. Jerome, *Solid St. Commun.*, **92**, 89–94 (1994).
12. C. Bourbonnais, and D. Jerome, *Advances in synthetic metals. Twenty Years of Progress in Science and Technology* (P. Bernier, S. Lefrant, and G. Bidan, eds) p. 206, Elsevier (1999).
13. Y. Suzumura, M. Tsuchiizu, and G. Gruner, *Phys. Rev. B*, **57**, R15040–15043 (1998).
14. V. Vescoli, L. Degiorgi, W. Henderson, G. Gruner, K. Starkey, and L. Montgomery, *Science*, **281**, 1181–1183 (1998).
15. D. S. Chow, F. Zamboroszky, B. Alavi, D. J. Tantillo, A. Bour, C. A. Merlic and S. E. Brown, *Phys. Rev. Lett*., **85**, 1698–1701 (2000).
16. F. Nad, P. Monceau, C. Carcel, and J. M. Fabre, *Phys. Rev. B*, **62**, 1753–1757 (2000).
17. P. Monceau, F. Y. Nad, and S. Brazovskii, *Phys. Rev. Lett.*, **86**, 4080–4083 (2001).
18. S. Mazumdar, S. Ramasesha, R. T. Clay, and D. K. Campbell, *Phys. Rev. Lett*., **82**, 1522–1525 (1999)
19. K. Hiraki, and K. Kanoda, *Phys. Rev. Lett.*, **82**, 2412–2415 (1999).
20. Y. Tomio, and Y. Suzumura, *J. Phys. Soc. Jap*., **69**, 796–801 (2000).
21. Y. Shibata, S. Nishimoto, and Y. Ohta, *Phys. Rev. B*, **64**, 235107–235111 (2001).
22. K. Ohno, *Theor. Chem. Acta*, **2**, 219–224 (1964); G. Klopmann, *J. Am. Chem. Soc.*, **86**, 4550–4554 (1964)
23. F. Mila, *Phys. Rev. B.*, **52**, 4788–4792 (1995).